Citation: Molecular Therapy—Nucleic Acids (2013) 2, e139; doi:10.1038/mtna.2013.66

www.nature.com/mtna

Influence of Polyethylene Glycol Lipid Desorption Rates on Pharmacokinetics and Pharmacodynamics of siRNA Lipid Nanoparticles

Barbara L Mui[1], Ying K Tam[1], Muthusamy Jayaraman[2], Steven M Ansell[1], Xinyao Du[1], Yuen Yi C Tam[3], Paulo JC Lin[3], Sam Chen[3], Jayaprakash K Narayanannair[2], Kallanthottathil G Rajeev[2], Muthiah Manoharan[2], Akin Akinc[2], Martin A Maier[2], Pieter Cullis[3], Thomas D Madden[1] and Michael J Hope[1]

Lipid nanoparticles (LNPs) encapsulating short interfering RNAs that target hepatic genes are advancing through clinical trials, and early results indicate the excellent gene silencing observed in rodents and nonhuman primates also translates to humans. This success has motivated research to identify ways to further advance this delivery platform. Here, we characterize the polyethylene glycol lipid (PEG-lipid) components, which are required to control the self-assembly process during formation of lipid particles, but can negatively affect delivery to hepatocytes and hepatic gene silencing *in vivo*. The rate of transfer from LNPs to plasma lipoproteins *in vivo* is measured for three PEG-lipids with dialkyl chains 14, 16, and 18 carbons long. We show that 1.5 mol % PEG-lipid represents a threshold concentration at which the chain length exerts a minimal effect on hepatic gene silencing but can still modify LNPs pharmacokinetics and biodistribution. Increasing the concentration to 2.5 and 3.5 mol % substantially compromises hepatocyte gene knockdown for PEG-lipids with distearyl (C18) chains but has little impact for shorter dimyristyl (C14) chains. These data are discussed with respect to RNA delivery and the different rates at which the steric barrier disassociates from LNPs *in vivo*.

Molecular Therapy—Nucleic Acids (2013) **2**, e139; doi:10.1038/mtna.2013.66; published online 17 December 2013
Subject Category: siRNA nanoparticles

Introduction

A new generation of highly potent, well-tolerated lipid nanoparticles (LNPs) for systemic delivery of short interfering RNA (siRNA) therapeutics has recently moved from research into human clinical testing with promising results.[1,2] RNA interference (RNAi) is a biological mechanism to control gene expression through silencing of mRNA transcripts. The discovery that RNAi can be induced by synthetic siRNAs designed to inhibit specific gene targets initiated extensive research into the development of therapeutics to silence the expression of previously "undruggable" proteins responsible for disease.[3] When siRNA is introduced into cells, specifically into cytoplasmic compartments, it may get loaded into RNA-induced silencing complex and direct sequence-specific cleavage of target mRNA. However, intracellular delivery of these large molecular weight, polyanionic compounds is a major challenge as they do not passively diffuse across plasma membranes. Several years ago it was discovered that siRNAs encapsulated in fusogenic, dialkyl amino LNPs potently inhibit hepatic gene expression *in vivo*, producing profound reductions in target protein levels for several weeks after a single dose.[4]

Rational molecular design has been applied to enhance the potency and safety of the amino lipid components,[5–7] and it was recently discovered that endogenous apolipoprotein E (Apo E) specifically targets these delivery systems to hepatocytes *in vivo* where they undergo Apo E–dependent, receptor mediated endocytosis.[8] The most advanced dialkyl amino LNP formulations are composed of four lipids. Two of these, cholesterol and saturated phosphatidylcholine, are considered structural components that do not appear to play a direct role in the mechanism of action. Amino lipid and polyethylene glycol lipid (PEG-lipid) components, on the other hand, play more active roles in both the formulation process and the mechanism of intracellular delivery. In previous studies, we defined the structure-activity relationship for dialkyl amino lipids with respect to hepatic gene silencing. Applying these molecular principles resulted in the synthesis of a highly active, novel amino lipid dilinoleylmethyl-4-dimethylaminobutyrate (DLin-MC3-DMA), which is referred to as MC3 and is the amino lipid used in the studies described here.[5] LNPs containing MC3 and encapsulating siRNA therapeutics are currently in Phase II clinical trials for hypercholesterolemia and transthyretin amyloidosis.[1,2] More recently, we have developed novel, next-generation lipids that combine the excellent potency of the most advanced lipids currently available with biodegradable functionality.[9]

In this work, we turn our attention to the PEG-lipid component of siRNA LNPs. PEG-lipids are typically incorporated into lipid-based drug delivery systems to provide a hydrophilic steric barrier that inhibits the binding of plasma proteins, including opsonins, which mark LNPs for removal by the mononuclear phagocytic system. The resulting increase in circulation lifetime enables drug delivery vehicles to take full advantage of enhanced permeability and retention effects, resulting in their accumulation at sites of disease.[10] However, PEG-lipid is incorporated into the current generation of siRNA LNPs for quite a different reason. Its primary role is to facilitate the self-assembly of LNPs by providing

[1]Acuitas Therapeutics, Vancouver, British Columbia, Canada; [2]Alnylam Pharmaceuticals, Cambridge, Massachusetts, USA; [3]Department of Biochemistry and Molecular Biology, University of British Columbia, Vancouver, British Columbia, Canada Correspondence: Michael J Hope, AcuitasTherapeutics, 407–2389 Health Sciences Mall, Vancouver, British Columbia, V6T 1Z4, Canada. E-mail: mhope@acuitastx.com
Key Words: drug delivery; hepatocyte; lipid nanoparticles; polyethylene glycol; siRNA; prenatal diagnosis
Received 11 October 2013; accepted 11 October 2013; advance online publication 17 December 2013. doi:10.1038/mtna.2013.66

a steric barrier at the surface of nascent particles formed when siRNA is rapidly mixed in acidic ethanol solutions with positively charged amino lipids. PEG steric hindrance prevents inter-particle fusion and promotes the formation of a homogeneous population of siRNA LNPs with diameters <100 nm.[11,12]

Yet the presence of a PEG shield on siRNA LNPs *in vivo* inhibits hepatic gene silencing activity. The protection it provides against interactions with plasma proteins appears to also interfere with Apo E-mediated endocytosis into hepatocytes.[8] Moreover, PEG-lipids reduce the close apposition and fusion required for the release of siRNA into the cytoplasm from endocytic vesicles.[13] Consequently, to maximize hepatic gene silencing *in vivo*, the concentration of PEG-lipid is reduced to the minimum required to support self-assembly and the alkyl chains are kept relatively short to promote shedding of the steric barrier following intravenous (i.v.) administration.

Given the important role of PEG-lipids in siRNA LNP delivery systems there is surprisingly little information available concerning their interactions with plasma after injection. Specifically, little is known about the kinetics of PEG release from LNPs *in vivo* or the identity of the PEG-lipid acceptors. Therefore, we conducted this study to characterize three PEG-lipids with saturated alkyl chain lengths of 14, 16, and 18 carbons. Dual labeled LNPs containing ^{14}C-MC3 and ^{3}H-PEG-lipid were employed to directly measure desorption rates for each chain length after separating LNPs from plasma lipoproteins. The desorption kinetics of the steric barrier were then correlated to LNP pharmacokinetics (PK), biodistribution (BD) and the ability to silence the hepatocyte-expressed factor VII gene.

Results

Dose and clearance of LNPs from blood

The objective of the first study was to determine the lipid dose at which to conduct this analysis. The current generation of siRNA LNPs is so potent that a typical therapeutic dose represents <1 mg/kg of total lipid injected i.v., of which only 3% by weight is PEG-lipid.[5] Taking into account the specific activities of ^{14}C- and ^{3}H-labeled lipids available, we estimated an siRNA dose administered at 0.3 mg/kg (3.3 mg/kg total lipid) would be sufficient to provide a limit of detection equivalent to ~1% of the injected dose per animal. Although this lipid dose is low for typical liposome drug delivery systems, it is still tenfold higher than that required for a therapeutic effect using siRNA LNPs in mouse models. Therefore, to ensure the data obtained in these studies is relevant to therapeutic applications, an experiment was conducted to compare the PK of LNPs at 0.03, 0.3, and 1.0 mg/kg siRNA.

LNPs encapsulating FVII siRNA were trace labeled with tritiatedcholesterylhexadecylether (^{3}H-CHE), an ether-linked cholesterol ester analogue. This lipid is nonexchangeable and nonmetabolizable in mice[14] therefore ^{3}H remains associated with particles in blood and tissues for at least 24 hours. LNPs were administered at total lipid doses of 0.33, 3.3, and 11.1 mg/kg (corresponding to 0.03, 0.3, and 1 mg/kg siRNA, respectively), and then blood, liver, and spleen samples were removed and measured for radioactivity over 24 hours. Expressed as % injected dose, all three concentrations show similar profiles for LNP clearance from the blood compartment and subsequent accumulation in liver and spleen tissues (**Figure 1**). Less than 5% of the injected dose remains in circulation after 4 hours and <1% after 24 hours (**Figure 1a**). The rates of accumulation by liver and spleen are also similar for the three doses, with 60–80% of the injected dose

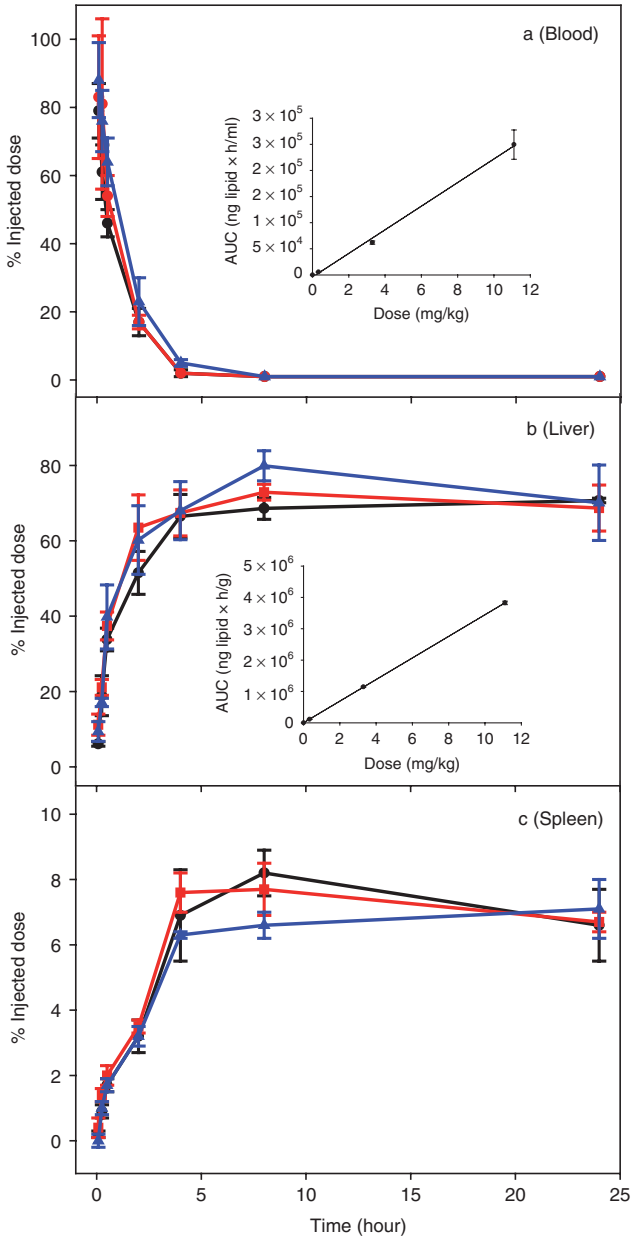

Figure 1 Plasma and tissue concentration-time profiles at different dose levels. LNPs containing 1.5 mol % PEG-C14 and trace ^{3}H-CHE were administered to mice at doses of 0.33 (circle), 3.3 (square), and 11.1 (triangle) mg/kg of lipid, equivalent to 0.03, 0.3, and 1 mg/kg siRNA, respectively. At various times, the animals were sacrificed and the amount of radiolabel present in blood, liver, and spleen was determined as outlined in Materials and Methods section. Dose proportionality is highlighted by the inserted linear plots of AUC (ng lipid·hour/g) versus lipid dose (mg/kg). Data points represent the average of 4 animals ± 1 SD. AUC, area under the curve; LNP, lipid nanoparticles; PEG, polyethylene glycol.

recovered in the liver (**Figure 1b**) and ~10% in the spleen (**Figure 1c**). These data, together with the corresponding PK values in **Table 1**, show the proposed siRNA dose of 0.3 mg/kg (total lipid dose of 3 mg/kg) falls within a range where dose proportionality is observed (linear area under the curve (AUC) versus lipid dose plots inserted into **Figure 1a**,**b**) with no indication that saturation of the mononuclear phagocytic system has been reached. Therefore, PK data obtained at this dose are expected to extrapolate to the therapeutic dose range.

Characterizing the ^{14}C-MC3 to ^{3}H-CHE ratio *in vivo*

In order to measure desorption rates of ^{3}H-PEG-lipids from LNPs, we intended to use ^{14}C-MC3 as the reference lipid that remains associated with LNPs in the circulation. To confirm its suitability, a dual label study was conducted, which showed the ratio of ^{14}C-MC3 to ^{3}H-CHE, a lipid known to stay associated with LNPs in the circulation, did not change over a 2-hour period *in vivo* (**Figure 2**). During this time, 90% of the injected LNP dose is removed from blood, therefore the disposition of PEG-lipids in the circulation was determined over a 0- to 2-hour time course.

Table 1 Pharmacokinetic parameters for mice administered siRNA LNPs containing 1.5 mol % PEG-C14

siRNA dose (mg/kg)[a]	$t_{1/2}$ (hour)[b]	Blood AUC$_{(0–24\ hour)}$ (μg lipid·hour/ml)	Liver AUC$_{(0–24\ hour)}$ (μg lipid·hour/g)
0.03	0.53 ± 0.12	5.6 ± 0.3	110.0 ± 3.5
0.30	0.71 ± 0.04	61.8 ± 3.2	1,145.7 ± 19.0
1.00	0.77 ± 0.05	249.4 ± 28.0	3,825.5 ± 55.5

AUC, area under the curve; LNP, lipid nanoparticles; PEG, polyethylene glycol.
[a]LNPs, trace labeled with ^{3}H-CHE, were administered i.v.at siRNA doses of 0.03, 0.3, and 1 mg/kg. [b]$t_{1/2}$ for LNP distribution from blood into tissues and AUCs for blood and liver were determined as described in Materials and Methods section. Data points represent the average of 4 mice ± 1 SD.

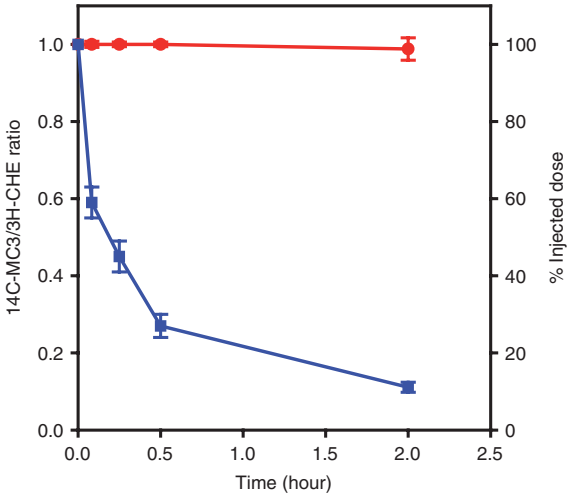

Figure 2 Comparison of ^{14}C-MC3 and ^{3}H-CHE as LNP markers. Mice, injected with LNPs containing 1.5 mol % PEG-C14, dual labeled with ^{14}C-MC3 and ^{3}H-CHE, were sacrificed at various times up to a maximum of 2 hours and the amount of radiolabel present in the blood determined as outlined in Materials and Methods section. The % injected dose was determined using ^{3}H-CHE (square) and the ^{14}C-MC3 to ^{3}H-CHE ratio (circle) was used to show ^{14}C-MC3 is a stable LNP marker for at least 2 hours after injection, during which time ~90% of the injected dose distributes out of the blood compartment. Data represent the average of 4 animals ± 1 SD. LNP, lipid nanoparticles; PEG, polyethylene glycol.

Desorption of PEG-lipids with different chain lengths from LNPs *in vivo*

The most common PEG-lipids employed in the current generation of siRNA LNPs contain two saturated, dimyristyl chains (PEG-C14).[7] We have shown *in vitro* that PEG-C14 transfers from LNPs to lipoproteins at a rate of ~50%/hour in mouse plasma at an LNP-to-plasma ratio equivalent to administering LNPs *in vivo* at a total lipid dose of 20 mg/kg, which is sevenfold higher than the dose employed here (manuscript in preparation). *In vivo*, a gradual increase in the ^{3}H/^{14}C ratio measured in whole blood and plasma occurs over the first hour indicating that ^{14}C-MC3–labeled LNPs are leaving the circulation faster (80% cleared in the first hour, **Figure 3a**), than ^{3}H-PEG-C14. These data are consistent with ^{3}H-PEG-C14 transferring to lipoproteins, which remain in circulation longer than LNPs, resulting in an increase in ^{3}H/^{14}C ratio. Specific loss of ^{3}H-PEG-lipid from LNPs becomes more apparent when plasma, isolated from blood drawn at each time point, is separated from lipoproteins by size exclusion chromatography enabling the ^{3}H/^{14}C ratio of the recovered LNPs to be measured directly (**Figure 3a**). The ratio decreases rapidly, with ~80% of the initial ^{3}H-PEG-C14 leaving LNPs within 2 hours.

The hydrophobic interactions responsible for associating PEG-lipids with LNP membranes are proportional to their alkyl chain length.[14,15] Therefore, PEG-C16 and PEG-C18 lipids should remain associated with LNPs *in vivo* longer than PEG-C14, as more energy is required for the longer chains to leave the membrane. Analysis of LNPs containing these lipids confirms this, with desorption estimated at 45, 1.3, and 0.2%/hour for C14, C16, and C18 PEG-lipids, respectively (**Figure 3b**).

The effect of PEG-lipid chain length and concentration on LNP pharmacodynamics

In the next series of experiments, we determine the effect of PEG chain length on murine hepatic gene silencing using FVII siRNA LNPs. Activity was measured over a range of doses which enables the determination of the dose required to reduce plasma FVII protein concentration by 50% (ED$_{50}$), for each formulation (**Figure 4**). We have shown previously that this represents the most accurate method to compare the potency of different formulations.[5,7] There is no statistically significant difference ($P > 0.05$) in the ED$_{50}$ values for LNPs containing 1.5 mole % PEG-C14, -C16, or -C18 (**Figure 4a**, ED$_{50}$ range 0.02–0.04 mg siRNA/kg). Increasing the concentration of PEG-C14 from 1.5 to 2.5 and 3.5 mol % results in ED$_{50}$ values for FVII silencing of 0.02, 0.03, and 0.06 respectively (**Figure 4b**), differences which are also not statistically significant. However, LNPs containing 2.5 and 3.5% PEG-C18 are inactive over the concentration range employed (**Figure 4c**).

The effect of PEG-lipid chain length on LNP PK and BD

Steric barriers provided by PEG-lipid are most commonly employed to reduce the rate at which drug delivery systems distribute from the blood compartment and to redirect their BD away from the liver.[10] Consequently, both PK and BD of LNPs can be modified by changing the anchor chain length of PEG-lipids.[14,16] This effect is shown for siRNA LNPs containing

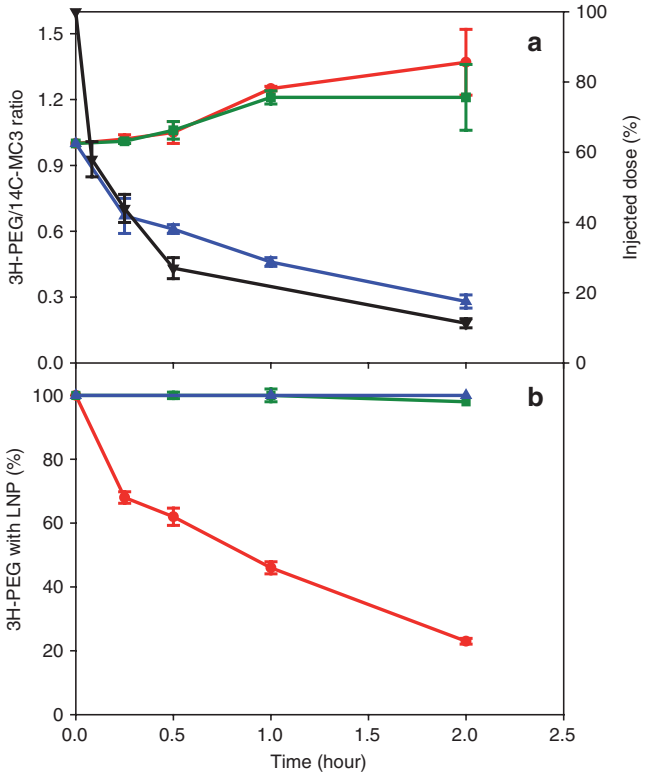

Figure 3 Loss of PEG-lipid from LNPs in circulation. (**a**) Mice injected with LNPs containing 1.5% mol % PEG-C14, dual labeled with ^{14}C-MC3 and ^{3}H-PEG-C14, were sacrificed at various times and the ^{3}H-PEG to ^{14}C-MC3 ratio determined in blood (circle), plasma (square), and LNP isolated from plasma (triangle) as outlined in Materials and Methods section. The clearance of the LNP as measured by ^{14}C-MC3 in the blood is shown as the percent injected dose (inverted triangle). (**b**) LNPs containing 1.5 mol % PEG-C14 (circle), PEG-C16 (square), or PEG-C18 (triangle), dual labeled with ^{14}C-MC3 and the corresponding ^{3}H-PEG-lipid were injected into mice. At various times the animals were sacrificed, plasma isolated and the amount of ^{3}H-PEG retained with LNPs measured as outlined in Materials and Methods section. Data represent the average of 4 animals ± 1 SD. LNP, lipid nanoparticles; PEG, polyethylene glycol.

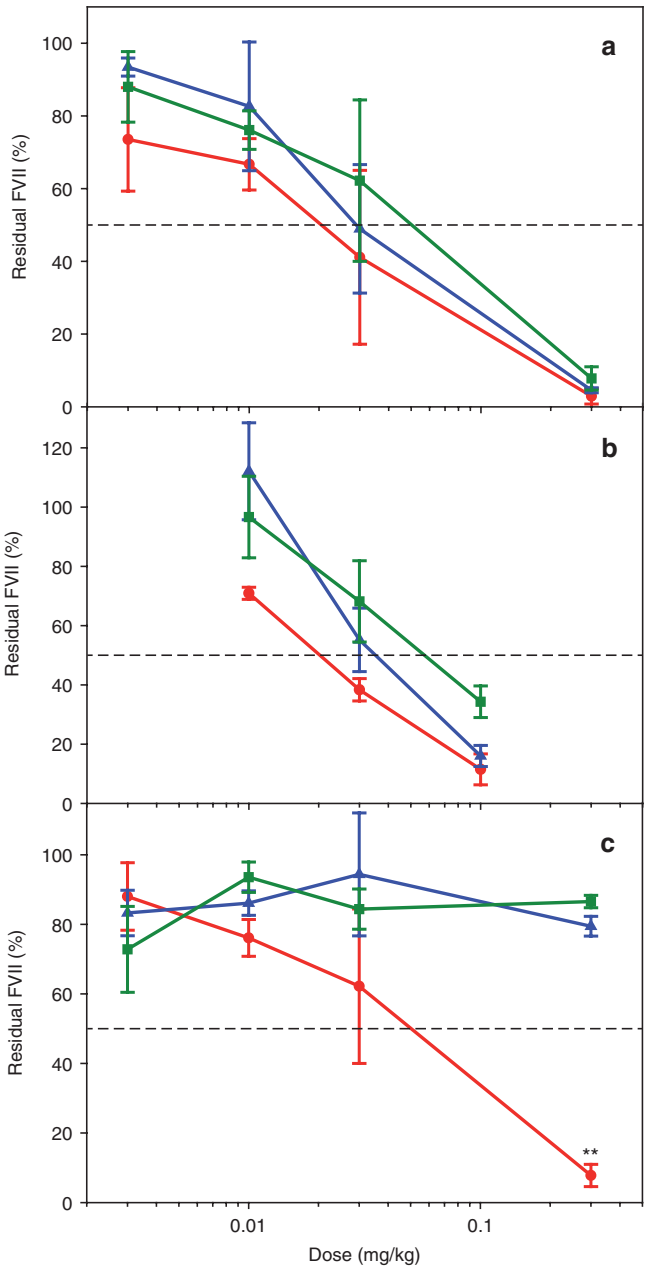

Figure 4 Effect of PEG-lipid on FVII gene silencing activity. (**a**) FVII siRNA LNPs containing 1.5 mol % PEG-C14 (circle), PEG-C16 (triangle), or PEG-C18 (square) were administered to mice at the indicated siRNA doses and plasma FVII protein concentrations determined 24 hours later. ED_{50}'s of 0.02, 0.03, and 0.04 mg/kg siRNA estimated for PEG-C14, PEG-C16, and PEG-C18 respectively are not significantly different ($P > 0.05$). (**b**) PEG-C14 content of 1.5 mol % (circle), 2.5% (triangle), and 3.5% (square) exhibit ED_{50}'s of 0.02, 0.03, and 0.06 mg/kg siRNA respectively, which are also not significantly different. (**c**) PEG-C18 content of 1.5 mol % (circle), 2.5% (triangle), and 3.5% (square) exhibit ED_{50}'s of 0.04, >0.3, and >0.3 mg/kg siRNA, respectively. The difference in activity observed at 1.5% PEG-C18 is statistically significant compared to 2.5 and 3.5% (**$P < 0.005$). Data points represent the average of 3–6 mice ± 1 SD. LNP, lipid nanoparticles; PEG, polyethylene glycol.

PEG-C14, -C16, and -C18 where both ^{3}H-PEG-lipid and ^{14}C-MC3 are tracked in blood, liver, and spleen over 24 hours (**Figure 5** and **Table 2**). Using ^{14}C-MC3 to track LNPs, the most rapid clearance of LNPs from blood is observed for PEG-C14 ($t_{1/2}$ = 0.64 hours), followed by PEG-C16 and -C18 LNPs with $t_{1/2}$ = 2.18 and 4.03 hours, respectively (**Figure 5a** and **Table 2**). The rate of ^{14}C-MC3 clearance from the blood compartment is not significantly different ($P > 0.05$) from that obtained for the same LNPs labeled with ^{3}H-CHE (see **Tables 1** and **2**), indicating that the MC3 lipid remains associated with LNPs while in circulation. This is also shown in **Figure 2**, where ^{14}C-MC3 remains associated with LNPs over 2 hours in circulation, during which time 90% of the particles are removed. In contrast, ^{3}H-PEG-C14 exhibits a longer $t_{1/2}$ and greater blood AUC than the ^{14}C-MC3 (**Figure 5b** and **Table 2**), consistent with the movement of this lipid into the lipoprotein pool, where it remains in circulation for longer.

Distribution out of the blood compartment for the three formulations correlates with concomitant accumulation in liver tissue (**Figure 5c**). PEG-C14 LNPs accumulate rapidly, reaching a maximum 55% of the injected dose at 4 hours. Note, however, that the total amount of PEG-C14 LNPs removed by liver tissue at this dose is actually 70%,

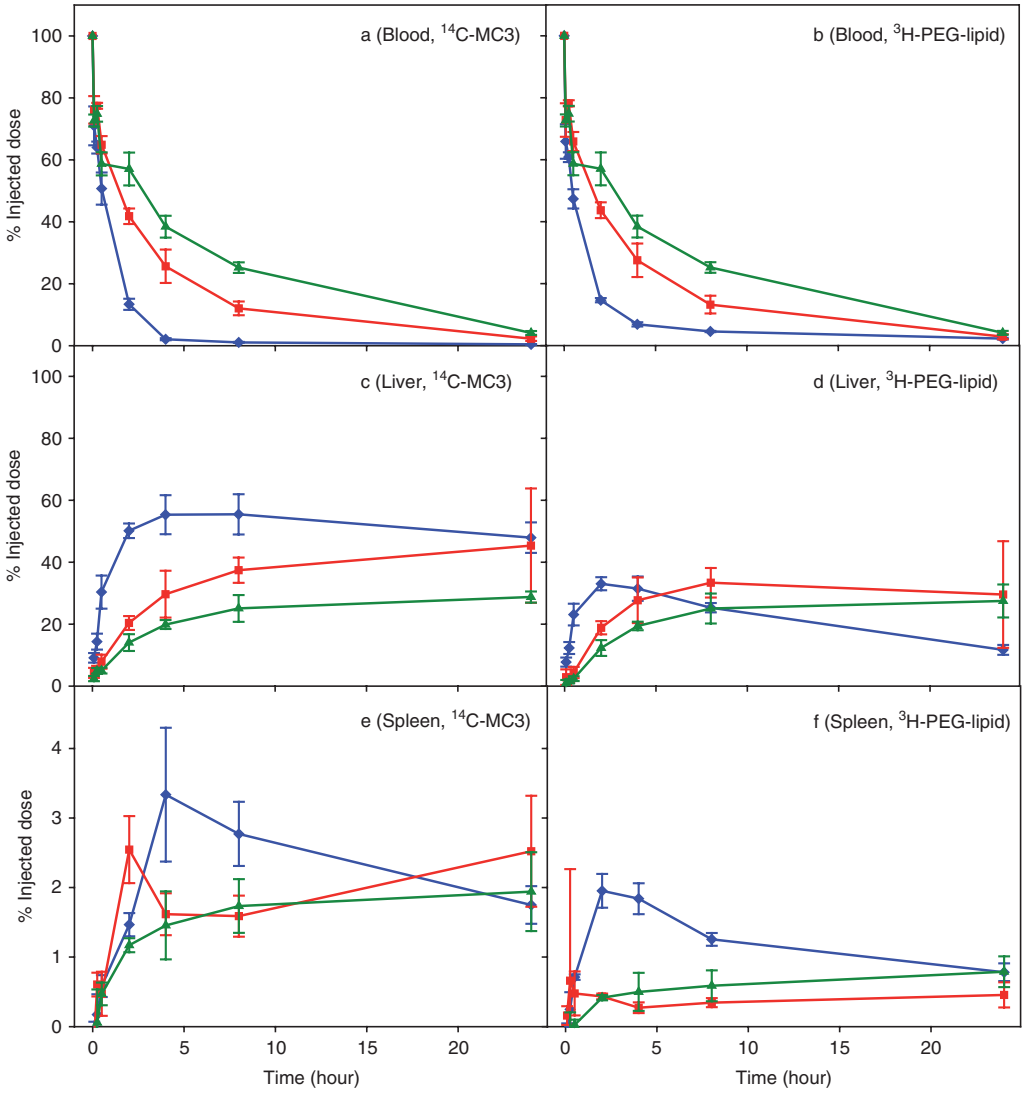

Figure 5 Effect of PEG-lipid chain length on pharmacokinetics and biodistribution. Mice were administered LNPs containing 1.5 mol % PEG-C14 (diamond), PEG-C16 (square), and PEG-C18 (triangle), dual labeled with ^{14}C-MC3 and the corresponding ^{3}H-PEG-lipids. At various times the animals were sacrificed and the concentration of ^{14}C and ^{3}H measured in blood, liver, and spleen. Data points represent the average of 4 mice ± 1 SD. LNP, lipid nanoparticles; PEG, polyethylene glycol.

Table 2 Pharmacokinetic parameters for mice administered siRNA LNPs containing 1.5 mol % C14, C16, and C18 PEG-lipids

	$t_{1/2}$ (hour)[b]		Blood $AUC_{(0–24\ hour)}$ (μg lipid·hour/ml)		Liver $AUC_{(0–24\ hour)}$ (μg lipid·hour/g)	
PEG-lipid[a]	^{14}C-MC3	^{3}H-PEG-lipid	^{14}C-MC3	^{3}H-PEG-lipid	^{14}C-MC3	^{3}H-PEG-lipid
PEG-C14	0.64 ± 0.08	0.91 ± 0.04	52.8 ± 2.0	105.6 ± 1.6	871.8 ± 46.0	486.7 ± 28.8
PEG-C16	2.18 ± 0.29	2.61 ± 0.30	166.8 ± 9.0	202.2 ± 12.8	566.6 ± 60.8	515.8 ± 72.7
PEG-C18	4.03 ± 0.37	4.60 ± 0.41	251.3 ± 9.0	270.8 ± 8.0	373.5 ± 33.1	359.1 ± 46.7

AUC, area under the curve; LNP, lipid nanoparticles; PEG, polyethylene glycol.
[a]LNPs, trace labeled with ^{14}C-MC3 and ^{3}H-PEG-lipid, were administered i.v.at an siRNA dose of 0.3 mg/kg. [b]$t_{1/2}$ for LNP distribution from blood into tissues (measured using the ^{14}C-MC3 label only) and AUCs for blood and liver for both radiolabels were determined as described in Materials and Methods section. Data points represent the average of 4 mice ± 1 SD.

determined using the stable lipid marker ^{3}H-CHE (**Figure 1b**). We speculate that it appears lower when measured using ^{14}C-MC3 as trace label because the ester between the ^{14}C-label and the alkyl chains is slowly hydrolyzed. This would also account for the lower $AUC_{(0–24)}$ for ^{14}C-MC3 in the liver, which is ~25% lower than that obtained using the nonexchangeable and nonmetabolizable ^{3}H-CHE label (**Tables 1** and **2**). An even lower liver accumulation is observed for the ^{3}H-PEG-C14, consistent with the rapid dissociation of this molecule from circulating LNPs as discussed above (**Figure 3a**). Peak accumulation occurs after 2 hours at just 30% of the injected dose (**Figure 5d**). Interestingly, there is also a steady

decline in ^{3}H-PEG-C14 recovered between 2 and 24 hours (**Figure 5d**), indicating that when this lipid is taken up by the liver it is either metabolized or excreted over time.

Both PEG-C16 and -C18 accumulate more slowly in the liver and only reach a maximum of 35 and 25% of the injected dose respectively (**Figure 5d** and **Table 2**). Moreover, the elimination of ^{3}H-PEG-lipid from the liver over 24 hours also appears to depend on chain length, with a large decrease in PEG-C14 levels between 2 and 24 hours compared to PEG-C16 and PEG-C18. These lipids have identical structures including ether linkages between the alkyl chains and headgroup that are resistant to hydrolysis.[17] Therefore, these data suggest that the rate of PEG-lipid elimination from liver tissue may depend on its hydrophobicity and ability to interact with biological membranes. When uptake is expressed in grams lipid/gram of tissue, the spleen removes equivalent amounts of LNPs as liver. However, the spleen is smaller and therefore distribution to this organ typically accounts for <10% of the injected dose. Although standard errors are larger for the spleen data, the trends with respect to PEG-lipid chain length and accumulation are similar to those observed in liver (**Figure 5e,f**).

Discussion

The steric barrier provided by PEG-lipid is necessary to control particle size during self-assembly of siRNA LNPs but has the negative attribute of inhibiting hepatic gene silencing *in vivo*.[7,8] In this study, we evaluate three PEG-lipids with dialkyl chains of 14, 16, and 18 carbons and correlate transfer rates with their effect on PK and activity *in vivo*. LNP delivery systems containing ionizable dialkylamino lipids require endogenous Apo E in order to access hepatocytes through Apo E–dependent, receptor mediated endocytosis. Therefore, one explanation for inhibition of activity is that PEG interferes with Apo E binding to LNPs.[8] However, it is also possible that a PEG shield prevents bound Apo E from undergoing the lipid-induced structural transition required for binding to hepatocyte receptors or the PEG barrier interferes with receptor recognition of Apo E on the LNP surface.[18,19] In this study, we characterize how a short chain PEG-lipid, with covalently attached PEG of molecular weight 2000, helps to mitigate this problem by rapidly exchanging from the LNP surface to plasma lipoproteins following i.v. administration. We evaluate three PEG-lipids with dialkyl chains of 14, 16, and 18 carbons and correlate transfer rates with their effect on PK and activity *in vivo*.

The spontaneous transfer of lipid from a membrane monolayer into the aqueous phase proceeds through a transition-state complex where the molecule is attached to the membrane by the tip of its hydrophobic tail.[20] The activation energy required to enter this state is very high and largely determined by the number and length of hydrophobic chains within the molecule. Lipids that achieve this transition state can rapidly diffuse through the aqueous space down a concentration gradient to acceptor sites such as other membranes and lipoproteins. The large energy barrier associated with entering the activated state is why the majority of membrane phospholipids, which have two acyl chain lengths >16 carbons, form stable bilayers and exhibit extremely low rates of transfer, with typical half-times of hundreds of hours in the absence protein facilitators.[20] The rate of lipid desorption, however, increases exponentially with decreasing chain length and is further enhanced by large hydrophilic headgroups, such as PEG, that contribute to lower the energy required to adopt transition-state complexes.[13,19]

By isolating plasma at various time intervals after injection and separating LNPs from lipoproteins, we determined the rate of loss for each PEG-lipid from LNPs *in vivo* to be >45%/hour, 1.3%/hour, and 0.2%/hour for C14, C16, and C18, respectively. Formulation optimization studies have consistently demonstrated that to form stable siRNA LNPs with diameters <100 nm the minimum amount of PEG_{2000}-lipid required is ~1.5 mol %.[5,7] At this concentration, FVII siRNA LNPs containing PEG-C14, -C16, and -C18 exhibit similar siRNA ED_{50}'s of ~0.03 mg/kg. When the PEG-lipid content is raised to 2.5 mol % there is little or no effect on the ED_{50} of PEG-C14 LNPs, whereas PEG-C18 LNPs completely lose activity in the dose range tested. This impact on activity resulting from such a small increase in mol percent highlights the effectiveness of the steric barrier provided by PEG-lipids.

The rate of PEG-C18 desorption from LNPs is 0.2% per hour, which is negligible relative to their circulation half-life of under 4 hours and consistent with the general assumption that PEG-C18 steric barriers can be considered permanently associated to circulating lipid-based delivery systems. Both theoretical and experimental data indicate that the concentration of PEG_{2000} required to completely cover both sides of model membrane bilayer surface is ~2–3 mol % of total lipid.[21,22] Below 1 mol % there is sufficient space between neighboring PEG clouds, or mushroom configurations, to allow large molecules access to the membrane surface. As the PEG concentration increases to 3 mol % the mushrooms are squeezed together to cover the whole surface, forming a cohesive PEG barrier. Between 3–10 mol % the increased PEG density causes the polymers to extend away from the membrane surface and adopt a brush configuration.[21] Recent data indicate that for siRNA LNPs all the PEG-lipid is located in the outer lipid monolayer,[23] therefore 1.5 mol % of total lipid would approximate 3 mol % of the outer monolayer lipid. Consequently, the abrupt change in siRNA LNP activity corresponds reasonably well to crossing the threshold between incomplete and complete coverage of the surface by PEG. It is also consistent with 1.5 mol % being the minimum PEG_{2000} concentration necessary to prevent particle-particle fusion during self-assembly.

The initial rate of desorption for PEG-C14 from LNPs *in vivo* is ~2% per minute, this slows down at later time points presumably because of back exchange from lipoproteins (**Figure 3b**). However, the rate of transfer to lipoproteins is fast enough to significantly mitigate the negative effect of the PEG shield on FVII knockdown at 2.5 and 3.5%. PK and BD data for siRNA LNPs indicate that the mechanism of LNP removal from the circulation does not exhibit the same PEG-lipid threshold effect as seen for hepatic gene silencing. At 1.5 mol % PEG-lipid the circulation half-life of ^{14}C-MC3–labeled LNPs (estimated over 24 hours) for PEG-C14, -C16, and -C18 LNPs is 0.64, 2.18, and 4.03 hours respectively. There is also a marked decrease in liver and spleen uptake with increasing chain length. These data indicate that both 1.5 mol % PEG-C16 and -C18 steric barriers reduce the association of opsonins with LNPs in the circulation. The reason for the

different PEG effects for opsonin induced clearance and Apo E-mediated uptake are not known at this time, but may reflect the molecular weights of the various proteins involved and their ability to penetrate a low density PEG shield.

Despite the differences in liver uptake between LNPs containing 1.5 mol % PEG-C14 and PEG-C18 they exhibit similar gene silencing activities, indicating that delivery to the liver alone is not a limiting factor for activity under these dosing conditions. As might be expected, a comparison of ^{14}C-MC3 to ^{3}H-PEG-lipid in liver shows that the amount of ^{3}H-label taken up reflects the rates of transfer to lipoproteins and erythrocytes while LNPs are in the circulation (**Figure 5c**,**d**). However, it is interesting to note that by 24 hours, >50% of the ^{3}H-PEG-C14 accumulated in the liver at 2 hours has been eliminated whereas the concentration of ^{3}H-PEG-C18 remains constant. The ^{3}H-label is located in the alkyl chains, which are joined to the headgroup by metabolically stable ether linkers.[17] Consequently, the differences in liver processing between the short and long chain PEG-lipids may also be related to lipid transfer rates and perhaps reflect PEG-C14 excretion into bile rather than metabolism. The % injected dose that distributes to the spleen is much less than the liver as it is a much smaller organ but the chain length trends are similar.

In summary, we demonstrate that the presence of a 1.5 mol % PEG_{2000}-lipid steric barrier does not significantly affect *in vivo* hepatic gene silencing for siRNA LNPs. However, increasing the PEG-lipid concentration by just 1 mol % can significantly reduce activity unless a short chain PEG-C14 is used, which rapidly desorbs from LNPs in the circulation and transfers to lipoproteins and erythrocytes. Moreover, different combinations of PEG-lipid chain length and concentration can be employed to modify the PK and BD of siRNA LNPs without greatly impacting hepatic gene silencing.

Materials and methods

General. Distearoylphosphatidylcholine and cholesterol were purchased from Avanti Polar Lipids (Alabaster, AL) and Sigma (St Louis, MO), respectively. The syntheses of MC3[5] and PEG-lipids[24] have been described previously. FVII siRNA was synthesized by Alnylam and characterized by electrospray mass spectrometry and anion exchange HPLC, the sequence has been presented elsewhere.[25]

Radiolabeled lipids. The PEG-lipid precursors containing one unsaturation in each of the lipid chains (myrystoleyl, palmetoleyl and oleyl chains, C14, C16, and C18 respectively) were synthesized using a similar procedure to that used for the synthesis of corresponding saturated analogs as reported.[24] ^{3}H-PEG-lipids (410 Ci/mol) were synthesized at Moravek-Biochemicals (Brea, CA) by catalytic reduction of the double bonds present in the lipid chains using tritium gas over Pd/C. Tritiatedcholesterylhexadecylether (^{3}H-CHE, 48,000 Ci/mol) was purchased from Perkin Elmer (Waltham, MA) and ^{14}C-MC3 (58 Ci/mol) was synthesized as described elsewhere.[6]

Preparation of LNP formulations. MC3, distearoylphosphatidylcholine, cholesterol and PEG-lipid were solubilized in ethanol at a molar ratio of 50:10:38.5:1.5. For LNPs containing 2.5 and 3.5% PEG-lipids, the cholesterol content was lowered to 37.5 and 36.5%, respectively. Radiolabeled lipids were included in the ethanolic lipid solution at a ^{3}H to ^{14}C dpm ratio of ~3 and their mass is taken into account in the target lipid mole ratios indicated above. The ^{3}H-CHE content was adjusted to 0.1, 0.02, and 0.006 mol % with respect to the total lipid for LNPs dosed at 0.33, 3.33, and 11.1 mg/kg lipid respectively. LNP specific activities were calculated to allow a minimum detection of ~1% of the injected dose per animal.

LNPs were prepared at a total lipid to siRNA weight ratio of ~10:1 as described elsewhere.[6] Briefly, the siRNA was diluted to 0.2 mg/ml in 10 mmol/l citrate buffer, pH 4. Syringe pumps were used to mix the ethanolic lipid solution with the siRNA aqueous solution at a 1:5 (vol/vol) ratio using pump rates of 6.8 and 34 ml/minute, respectively. The two syringes containing the siRNA and lipid solutions were connected to a union connector (IDEX Health & Science #P-728) with PEEK HPLC tubing (0.02 inch ID for siRNA solution and 0.01 inch ID for lipid solution). A length of PEEK HPLC tubing (0.04 inch ID) was connected to the outlet of the union connector and led to a collection tube. The ethanol was then removed and the external buffer replaced with phosphate-buffered saline (155 mmol/l NaCl, 3 mmol/l Na_2HPO_4, 1 mmol/l KH_2PO_4, pH 7.5) by dialysis. Finally, the LNPs were filtered through a 0.2 µm pore sterile filter. LNP particle size was 70–90 nm diameter as determined by quasi-elastic light scattering using a Nicomp370 submicron particle sizer (Santa Barbara, CA). Lipid concentrations were calculated based on the total cholesterol measured using the cholesterol E enzymatic assay kit from Wako Chemicals (Richmond, VA). SiRNA content was determined by A260 after solubilizing an aliquot in a chloroform:methanol:aqueous mixture (final volume ratio of 1:2.1:1). Removal of free siRNA was performed using VivaPureDMiniH columns (Sartorius Sedim Biotech, Goettingen, Germany). Encapsulation efficiency was determined from the ratio of siRNA before and after removal of free siRNA content, normalized to lipid content.

PK and BD of radiolabeled LNP. Radiolabeled LNPs were administered intravenously via the lateral tail vein at a volume of 10 ml/kg in 6- to 8-week-old CD-1 mice. At various times, the mice were anesthetized with Ketamine/Xylazine and blood withdrawn by cardiac puncture and collected in microtainer tubes with EDTA (Becton-Dickinson, Franklin Lakes, NJ). A portion of the blood was centrifuged at 500*g* for 10 minutes to isolate plasma. Liver and spleen tissue were also processed by transferring the pre-weighed whole spleen or a piece of the liver (60–80 mg) into Fastprep tubes and homogenized with phosphate-buffered saline (0.75–1 ml) using a Fastprep-24 (MP Biomedical, Santa Ana, CA). Aliquots (0.1–0.2 ml) of the homogenate, blood, and plasma were transferred to 7 ml glass scintillation vials and subjected to a digestion and decolorization protocol as follows. An aliquot (0.5 ml) of Solvable (Perkin Elmer, Waltham, MA) was added to the vial and the sample digested for 2 hours at 60 °C, after which the samples were cooled before adding 30% hydrogen peroxide (0.2 ml), 200 mmol/l EDTA (0.05 ml), and 10 N hydrochloric acid (0.025 ml). The mixture was decolorized overnight prior to adding 5 ml of PicoFluorPlus scintillation fluid (Perkin Elmer). Radioactivity was measured using a Beckman Coulter LS6500 liquid scintillation counter (Mississauga, Ontario, Canada). The percent recovery in blood and plasma

was calculated based on a volume of 70 and 38.5 ml/kg animal weight, respectively. Liver and spleen associated radioactivity are expressed as percent injected dose per total organ weight. Encapsulated siRNA was not followed in this study, but previous reports have shown that similar formulations do not leak nucleic acid in the circulation.[7,26]

PK and statistical analysis. AUC_{0-24} was calculated using the trapezoidal rule. The half-life for LNP and/or label distribution from the blood compartment into tissues was calculated by fitting the concentration versus time curve to first order exponential function $C_t = C_0 e^{(-kt)}$, where C_t and C_0 are the radiolabel concentrations at time t and zero. The distribution constant k derived from the plot was used to calculate $t_{1/2}$ using the formula $t_{1/2} = 0.693/k$. Statistical significance ($P \leq 0.05$) between data sets was determined using the Excel TTEST function.

Size exclusion chromatography to determine the rate of 3H-PEG-lipid transfer from LNPs to lipoproteins in vivo. The separation of LNPs from plasma lipoproteins using size exclusion chromatography has been described previously.[27] Loss of ^{3}H-PEG-lipid from ^{14}C-MC3–labeled LNP in plasma was determined using Sepharose CL-4B (Sigma) and 1.5 cm diameter × 30 cm columns. Plasma samples (0.2 ml) were eluted with phosphate-buffered saline and 20 × 2 ml fractions collected then mixed with 4.8 ml of PicoFluorPlus scintillation fluid and counted for radioactivity.

In vivo efficacy studies characterizing FVII gene silencing. Six- to eight-week-old female C57Bl/6 mice were obtained from Charles River Laboratories (Wilmington, MA). LNPs were diluted to the required concentrations in sterile phosphate-buffered saline before use and administered intravenously via the lateral tail vein at a volume of 10 ml/kg. After 24 hours, animals were anesthetized with Ketamine/Xylazine and blood collected by cardiac puncture. Samples were processed to serum using microtainer serum separator tubes (Becton-Dickinson) and stored at –70 °C for later analysis of FVII protein content using the colorimetric Biophen VII assay kit (Aniara, West Chester, OH). All procedures were approved by the University of British Columbia institutional animal care committee and performed in accordance with guidelines established by the Canadian Council of Animal Care.

The determination of FVII ED_{50} values has been described in detail elsewhere.[7] Briefly, formulations were administered over a range of siRNA doses chosen to include data points within 10–90% residual FVII activity (typically three to four points). ED_{50} values represent the siRNA dose in mg/kg at which the serum concentration of FVII has been reduced by 50% compared to the saline-control treated animals and is derived from a linear interpolation of the FVII activity profile as shown in **Figure 4**.

Conflict of interest. The authors are either employees of Acuitas Therapeutics or Alnylam Pharmaceuticals or have received research funding from these companies.

1. Coelho, T, Adams, D, Silva, A, Lozeron, P, Hawkins, PN, Mant, T *et al.* (2013). Safety and efficacy of RNAi therapy for transthyretin amyloidosis. *N Engl J Med* **369**: 819–829.
2. Fitzgerald, K, Frank-Kamenetsky, M, Shulga-Morskaya, S, Liebow, A, Bettencourt, BR, Sutherland, JE *et al.* (2013). Effect of an RNA interference drug on the synthesis of proprotein convertase subtilisin/kexin type 9 (PCSK9) and the concentration of serum LDL cholesterol in healthy volunteers: a randomised, single-blind, placebo-controlled, phase 1 trial. *Lancet.*
3. de Fougerolles, A, Vornlocher, HP, Maraganore, J and Lieberman, J (2007). Interfering with disease: a progress report on siRNA-based therapeutics. *Nat Rev Drug Discov* **6**: 443–453.
4. Zimmermann, TS, Lee, AC, Akinc, A, Bramlage, B, Bumcrot, D, Fedoruk, MN *et al.* (2006). RNAi-mediated gene silencing in non-human primates. *Nature* **441**: 111–114.
5. Jayaraman, M, Ansell, SM, Mui, BL, Tam, YK, Chen, J, Du, X *et al.* (2012). Maximizing the potency of siRNA lipid nanoparticles for hepatic gene silencing in vivo. *Angew Chem Int Ed Engl* **51**: 8529–8533.
6. Maier, MA, Jayaraman, M, Matsuda, S, Liu, J, Barros, S, Querbes, W *et al.* (2013). Biodegradable lipids enabling rapidly eliminated lipid nanoparticles for systemic delivery of RNAi therapeutics. *Mol Ther* **21**: 1570–1578.
7. Semple, SC, Akinc, A, Chen, J, Sandhu, AP, Mui, BL, Cho, CK *et al.* (2010). Rational design of cationic lipids for siRNA delivery. *Nat Biotechnol* **28**: 172–176.
8. Akinc, A, Querbes, W, De, S, Qin, J, Frank-Kamenetsky, M, Jayaprakash, KN *et al.* (2010). Targeted delivery of RNAi therapeutics with endogenous and exogenous ligand-based mechanisms. *Mol Ther* **18**: 1357–1364.
9. Maier, MA, Jayaraman, M, Matsuda, S, Liu, J, Barros, S, Querbes, W *et al.* (2013). Biodegradable lipids enabling rapidly eliminated lipid nanoparticles for systemic delivery of RNAi therapeutics. *Mol Ther* **21**: 1570–1578.
10. Allen, TM and Cullis, PR (2013). Liposomal drug delivery systems: from concept to clinical applications. *Adv Drug Deliv Rev* **65**: 36–48.
11. Maurer, N, Wong, KF, Stark, H, Louie, L, McIntosh, D, Wong, T *et al.* (2001). Spontaneous entrapment of polynucleotides upon electrostatic interaction with ethanol-destabilized cationic liposomes. *Biophys J* **80**: 2310–2326.
12. Semple, SC, Klimuk, SK, Harasym, TO, Dos Santos, N, Ansell, SM, Wong, KF *et al.* (2001). Efficient encapsulation of antisense oligonucleotides in lipid vesicles using ionizable aminolipids: formation of novel small multilamellar vesicle structures. *Biochim Biophys Acta* **1510**: 152–166.
13. Song, LY, Ahkong, QF, Rong, Q, Wang, Z, Ansell, S, Hope, MJ *et al.* (2002). Characterization of the inhibitory effect of PEG-lipid conjugates on the intracellular delivery of plasmid and antisense DNA mediated by cationic lipid liposomes. *Biochim Biophys Acta* **1558**: 1–13.
14. Semple, SC, Harasym, TO, Clow, KA, Ansell, SM, Klimuk, SK and Hope, MJ (2005). Immunogenicity and rapid blood clearance of liposomes containing polyethylene glycol-lipid conjugates and nucleic Acid. *J Pharmacol Exp Ther* **312**: 1020–1026.
15. Silvius, JR and Zuckermann, MJ (1993). Interbilayer transfer of phospholipid-anchored macromolecules via monomer diffusion. *Biochemistry* **32**: 3153–3161.
16. Parr, MJ, Ansell, SM, Choi, LS and Cullis, PR (1994). Factors influencing the retention and chemical stability of poly(ethylene glycol)-lipid conjugates incorporated into large unilamellar vesicles. *Biochim Biophys Acta* **1195**: 21–30.
17. Heyes, J, Hall, K, Tailor, V, Lenz, R and MacLachlan, I (2006). Synthesis and characterization of novel poly(ethylene glycol)-lipid conjugates suitable for use in drug delivery. *J Control Release* **112**: 280–290.
18. Mahley, RW and Huang, Y (2007). Atherogenic remnant lipoproteins: role for proteoglycans in trapping, transferring, and internalizing. *J Clin Invest* **117**: 94–98.
19. Nguyen, D, Dhanasekaran, P, Phillips, MC and Lund-Katz, S (2009). Molecular mechanism of apolipoprotein E binding to lipoprotein particles. *Biochemistry* **48**: 3025–3032.
20. Phillips, MC, Johnson, WJ and Rothblat, GH (1987). Mechanisms and consequences of cellular cholesterol exchange and transfer. *Biochim Biophys Acta* **906**: 223–276.
21. Kenworthy, AK, Hristova, K, Needham, D and McIntosh, TJ (1995). Range and magnitude of the steric pressure between bilayers containing phospholipids with covalently attached poly(ethylene glycol). *Biophys J* **68**: 1921–1936.
22. Torchilin, VP (1994). Immunoliposomes and PEGylated immunoliposomes: possible use for targeted delivery of imaging agents. *Immunomethods* **4**: 244–258.
23. Leung, AK, Hafez, IM, Baoukina, S, Belliveau, NM, Zhigaltsev, IV, Afshinmanesh, E *et al.* (2012). Lipid Nanoparticles Containing siRNA Synthesized by Microfluidic Mixing Exhibit an Electron-Dense Nanostructured Core. *J Phys Chem C Nanomater Interfaces* **116**: 18440–18450.
24. Akinc, A, Zumbuehl, A, Goldberg, M, Leshchiner, ES, Busini, V, Hossain, N *et al.* (2008). A combinatorial library of lipid-like materials for delivery of RNAi therapeutics. *Nat Biotechnol* **26**: 561–569.
25. Akinc, A, Goldberg, M, Qin, J, Dorkin, JR, Gamba-Vitalo, C, Maier, M *et al.* (2009). Development of lipidoid-siRNA formulations for systemic delivery to the liver. *Mol Ther* **17**: 872–879.
26. Tabernero, J, Shapiro, GI, LoRusso, PM, Cervantes, A, Schwartz, GK, Weiss, GJ *et al.* (2013). First-in-humans trial of an RNA interference therapeutic targeting VEGF and KSP in cancer patients with liver involvement. *Cancer Discov* **3**: 406–417.
27. Rodrigueza, WV, Pritchard, PH and Hope, MJ (1993). The influence of size and composition on the cholesterol mobilizing properties of liposomes in vivo. *Biochim Biophys Acta* **1153**: 9–19.